



A linearized transmission expansion planning model under $N - 1$ criterion for enhancing grid-scale system flexibility via compressed air energy storage integration

Hesam Mazaheri¹  | Moein Moeini-Aghaie²  | Mahmud Fotuhi-Firuzabad³  |

Payman Dehghanian⁴  | Mohammad Khoshjahan¹ 

¹ Department of Electrical and Computer Engineering, Texas A&M University, College Station, Texas, USA

² Department of Energy Engineering, Sharif University of Technology, Tehran, Iran

³ Department of Electrical Engineering, Sharif University of Technology, Tehran, Iran

⁴ Department of Electrical and Computer Engineering, The George Washington University, Washington, District of Columbia, USA

Correspondence

Mahmud Fotuhi-Firuzabad, Tehran 11365-11155, Iran.

Email: fotuhi@sharif.edu

[Correction added on 18-November-2021, after first online publication: Affiliation of Hesam Mazaheri is updated in this version of paper]

Abstract

The concept of flexibility is defined as the power systems' ability to effectively respond to changes in power generation and demand profiles to maintain the supply–demand balance. However, the inherent flexibility margins required for successful operation have been recently challenged by the unprecedented arrival of uncertainties, driven by constantly changing demand, failure of conventional units, and the intermittent outputs of renewable energy sources (RES). Tackling these challenges, energy storage systems (ESS) as one important player of the new power grids can enhance the system flexibility. It, therefore, calls for an efficient planning procedure to ensure flexibility margins by considering ESS's role in modern power systems. This paper proposes a novel mixed integer linear programming (MILP) model for transmission expansion planning (TEP) framework taking into account the role of compressed air energy storage (CAES) integration on improvements in system flexibility. The proposed framework is housed with a quantitative metric of grid-scale system flexibility, while a new offline repetitive mechanism is suggested to account for the $N - 1$ reliability criterion. The model is applied to different test systems, where the numerical results demonstrate the impacts of CAES units on system flexibility, investment plans, and the total costs.

1 | INTRODUCTION

Widespread integration of renewable energy sources (RES), wind and solar in particular, has recently resulted in the unprecedented presence of uncertainties in power grids, leading to transmission lines congestion and load curtailments [1–3]. The systems' ability to effectively cope with and control such fast- and slow-dynamic variations in generated power electricity and load demand is called power grid flexibility [1,4]. In fact, the system flexibility which captures both technical and economic objectives should be effectively addressed in the planning and operation decisions [1]. In order to techno-economically cope with the intermittency in RES, transmission expansion planning (TEP) [5] paradigms have put forward new plans to simultaneously ensure power grid economics, system flexibility, and reliability requirements. In addition, new investment plans

focused on various sources such as distributed energy resources, switching operations, HVDC lines, aggregated electric vehicles, demand-side management programs, and energy storage systems (ESS) have been investigated [2,4,6–9].

ESS, if planned and operated effectively, can unlock huge advantages in large-scale power grids as they alleviate the full reliance on the conventional generators, enhance the grid economics, mitigate transmission lines congestion scenarios, increase the usage of RES's capacities, and enhance the grid resilience during emergencies. Among the various ESS technologies, pumped hydro energy storage (PHES), compressed air energy storage (CAES), and battery energy storage systems (BESS) are the most implemented in large-scale generation/transmission systems.

Among PHES and smaller-size ESS technologies such as CAES and BESS, the latter alternatives are more practical owing

This is an open access article under the terms of the [Creative Commons Attribution](https://creativecommons.org/licenses/by/4.0/) License, which permits use, distribution and reproduction in any medium, provided the original work is properly cited.

© 2021 The Authors. *IET Generation, Transmission & Distribution* published by John Wiley & Sons Ltd on behalf of The Institution of Engineering and Technology

to lower construction costs [10,11]. Although both PHES and CAES technologies have geographical constraints, PHES would need to be constructed in remote sites with two reservoirs and pump units as compared to the CAES technology [12]. Therefore, CAES can be considered as more installable technology with lower geographical constraints. Furthermore, BESS technology reveals limitations in the number of charging or discharging cycles [6], while CAES remains an efficient and economic choice by providing additional required flexibility services. Compared to BESS, CAES technology is a more reliable source in large-scale power grids in terms of economic aspects. Although CAES units' installation depends on underground geological voids, the need to install many CAES units at each bus is relaxed due to CAES's capacity that stores higher capacity power for a long duration in comparison with BESS technology. In addition, CAES technology is found to be more efficient in power grids majorly composed of thermal generators—the case that this paper examined—while the integration of other ESS technologies may result in promising operational benefits in RES-rich power grids. We have tried to focus on the role of ESS technologies on the system flexibility as one important player of modern power systems. In this vein, the analyses of this paper are focused on ESS-integrated power systems with conventional generating units despite the generality of the proposed model. Considering the applications of CAES technology, a project is currently in operation by the *Iowa Association of Municipal Utilities* [11].

A stream of literature exists on the TEP planning and the integration of ESS units in power grids. Reference [13] proposes a mixed integer AC model for TEP by applying the conic relaxation of the optimal power flow. In this research, the disjunctive programming technique is extended to consider the power flow and the voltage constraints. A non-linear TEP model is presented in [14] with the impacts of ESS technologies on the investment and operation costs. In [15], an adaptive robust optimization model is suggested aiming to minimize the ESS-integrated TEP investment and achieve an effective operation under a wide range of uncertainties such as future generation, peak loads, and operational conditions. Authors in [9] present a long-term stochastic mixed integer linear programming (MILP) model to incorporate flexible network technologies into the TEP problem, further solved by the Benders decomposition scheme. In [16], a probabilistic TEP model is presented including load and wind uncertainties solved by the Benders decomposition and Monte Carlo simulation. To minimize the expansion plan cost as well as the load curtailment, a robust optimization TEP approach is proposed in [17] considering the uncertainties in the net injections. Reference [18] tries to present a renovated MILP robust model of TEP to address the uncertainties generated from the estimated transmission lines investment cost and the forecasted loads. Authors in [19] try to define a stochastic, multi-stage, co-planning model of TEP and BESS to improve power grid flexibility in dealing with uncertainties. A multi-stage MILP model is proposed in [20] including transmission and ESS planning under long-term uncertainties to improve a new metric of power system flexibility. Finally, reference [21] presents an MILP model for co-planning of trans-

mission networks and CAES units to defer transmission lines investment through an online method capturing the $N - 1$ reliability criterion. However, improvement in power grid flexibility was not the primary concern in [21].

Considering flexibility metrics and performance requirements, the authors in [6] provide a review on the concept, metrics, and implementation practices. Authors in [22–24] present new flexibility metrics as well as flexibility dynamics to be quantified in long-term system planning and real-time operation decisions. In [25], a systematic approach is defined to incorporate flexibility measures in generation planning and market operation. A robust optimization model is employed in [26] to quantify the long-term planning and short-term operation metrics of flexibility. Reference [1] suggests a novel techno-economic flexibility metric in day-ahead electricity markets. This paper has quantified the relative flexibility based on conventional generation technologies compared to modern flexible options such as ESS and demand response programs. To measure the power grid flexibility, authors in [27] try to present a novel adaptive robust optimization model under a unit commitment time-scale framework considering wind uncertainty. Finally, a five-level MILP optimization model for TEP is proposed in [28] under generation expansion uncertainty considering flexible network technologies and $N - 1$ security criterion.

In many of the above-mentioned literature, authors have employed non-linear and linear optimization models to assess the impacts of ESS integration on TEP, in which some solution techniques have been offered such as the genetic algorithm [14], the Benders decomposition scheme [9,16], and direct optimization method [21]. However, none has concentrated on the joint TEP and ESS planning in order to primarily improve metrics of system flexibility considering the ESS impacts. Although the solutions proposed in some of the existing literature indirectly and conceptually improve the system flexibility, the state-of-the-art literature (i) has neither defined nor measured any metric to demonstrate numerically the improvements in system flexibility by the planning solutions, and (ii) has not approached harnessing the available metrics of flexibility in a co-planning framework. Note that the presented design and formulations of CAES units have not been studied in the ESS-focused TEP problems. Finally, some references presented online methods to consider $N - 1$ security criterion [21], where the computationally-intensive optimization methods would not be efficient to solve the flexibility problem, which further motivates defining a novel offline approach to account for the $N - 1$ criterion.

To bridge the aforementioned gaps in the literature, an MILP direct-solution optimization model is presented that simultaneously captures both Transmission and CAES units' expansion in order to enhance the grid-scale system flexibility via ESS integration. Relaxing the need to use decomposition approaches, a novel techno-economic metric is suggested to quantify the system flexibility. Moreover, to mitigate the computational burden in solving the proposed problem, a novel offline mechanism is suggested to assess the $N - 1$ reliability criterion and ensure the power grid security in facing credible contingencies.

Consequently, the main contributions of this paper can be summarized as follows:

A novel techno-economic metric is suggested to numerically characterize the grid-scale system flexibility aided by the large-scale integration of CAES units.

A new MILP co-optimization framework is suggested for joint transmission and CAES expansion where accurate CAES design characteristics are incorporated considering the details of cost and energy levels.

An efficient linearization method with a direct and computationally-efficient solution technique is applied to the proposed MILP optimization model capturing the trade-offs between the TEP and the CAES units planning in large-scale power systems, being generic to accommodate other ESS technologies.

A novel and efficient offline mechanism is suggested to continuously assess the $N - 1$ reliability criterion that is independently calculated from the investment problem and enhances the solution feasibility.

The remainder of this paper is organized as follows. Section 2 introduces a big picture of the proposed algorithm. Problem formulation including the linearized model of TEP and CAES units, the grid-scale system flexibility assessment, and the $N - 1$ criterion is presented in Section 3. Sections 4 and 5 discuss the case study analysis, numerical results and discussion on the GARVER and the IEEE RTS test systems, respectively. Finally, the concluding remarks are presented in Section 6.

2 | PROPOSED ALGORITHM

The objective function in the proposed framework is defined as a three-stage optimization model to minimize the investment as well as the operation and maintenance costs of the installed transmission lines and the integrated CAES units. According to Figure 1, **Step 1** presents a linearized optimization model for TEP considering CAES units' integration. In order to linearize the non-linear TEP formulation, the well-known Big-M method is applied; also, an innovative approach is presented to linearize the non-linear CAES units' formulations. Therefore, a two-stage optimization model in which the Master problem focuses on the planning and the sub-problem on the operation can be converted to a single MILP optimization model to easily solved by linearization approaches. In this regard, power balance, power flow, power generation, and CAES units power and energy constraints are satisfied by decision variables based on the installed transmission lines and the integrated CAES units; then, a new flexibility metric is suggested to assess the grid-scale system flexibility and investigate the CAES units' positive influences on the power grid flexibility concept.

In **Step 2**, to satisfy the proposed model under contingencies, a practical and computationally-efficient offline mechanism is measured to repetitively assess the $N - 1$ reliability criterion which is independently calculated from the investment problem. With the investment plans found, load curtailment powers are

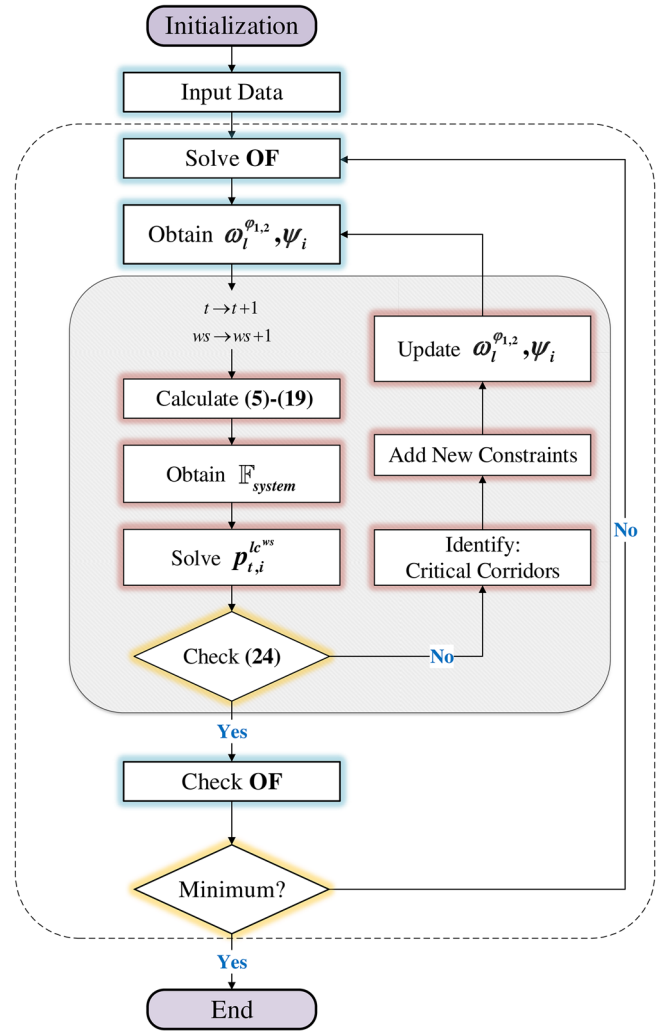


FIGURE 1 Flowchart of the proposed algorithm

evaluated when removing each of the available or the installed transmission lines in each corridor. Thus, if the load curtailment power in one scenario is greater than the corresponding limits, the system alerts as an emergency operating state and the critical corridors, which are more vulnerable than the others, are recognized. Then, a new constraint related to these corridors for the corresponding TEP plan is then added to the formulations. As a result, decision variables and then, the total cost are updated according to the contingency scenarios. This process is repeated to consider all contingencies and to satisfy the system security under contingency scenarios. When the system security is evaluated, the process of finding the investment plans is repeated to minimize the total cost.

The maximum number of transmission lines to be installed in each corridor is supposed to be two. Although the sizing of the integrated CAES units at each bus can be handled by the proposed method, the maximum number of CAES units to be integrated at each bus is assumed to be one due to the geographical constraints and the mechanical limitations of ESS (such as PHES and CAES) [11,29]. It should be noted that installing more than one unit at each bus may not be feasible in

practice. To consider the available transmission lines, one binary parameter is defined; in addition, the linearization method mandates the decision variables of installable transmission lines to be binary variables; as a result, we define another two binary variables to consider the maximum number of installable transmission lines in each corridor. Furthermore, two datasets corresponding to sample winter/summer days are considered in the operation sub-problem to simulate weather conditions throughout one target year in the proposed static co-planning structure [30]. This paper categorized investment plan variables, CAES units charging and discharging statuses, and CAES units linearizing variables as binary variables, while the output power of generating units, power flows through transmission lines, voltage phase angles, CAES units charging and discharging powers as well as energy level, the flexibility index, and the load curtailment power are categorized as continuous variables.

3 | PROBLEM FORMULATION

3.1 | Objective function

To structure the proposed MILP model considering the system flexibility improvement in CAES-integrated power grids, the objective function (OF) is comprised of two separate parts, that is the investment cost and the operation cost (1):

$$\mathbf{OF} = \min \left\{ C_{pl} + C_{op}^{ws} \right\} \quad (1)$$

$$C_{pl} = \sum_{l=1}^L \alpha_l^I \cdot \omega_l^{\varphi_{1,2}} + \sum_{i=1}^I \psi_i \cdot \left(\alpha^p \cdot \bar{p}_i + \alpha^e \cdot \bar{e}_i + \alpha^f \cdot \bar{p}_i \right) \quad (2)$$

$$C_{op}^{ws} = \sum_{ws=1}^Y f^{dsc} \zeta^{ws} \sum_{t=1}^T \sum_{i=1}^I \left(\alpha_i^g \cdot \bar{p}_{t,i}^{g,ws} + \alpha_t^{el} \cdot \bar{p}_{t,i}^{-ws} + \alpha^v \cdot \bar{p}_{t,i}^{+,ws} + \alpha^{ng} \cdot r^b \cdot \bar{p}_{t,i}^{q,ws} \right) \quad (3)$$

$$f^{dsc} = \sum_{n=1}^N \frac{1}{(1 + r^{dsc})^{n-1}} \quad (4)$$

The costs of the installed transmission lines, the integrated CAES units, and the fixed maintenance cost are evaluated in (2). Moreover, the system operation cost including the cost of the generated power from generating units, the CAES units' electricity consumption cost, variable maintenance cost, and natural gas consumption cost are presented in (3). Note that the second and fourth parts of the operation cost are the special terms in the CAES technology calculation, differentiated from other types of ESS technologies. The heat rate parameter r^b in (3) is specifically defined for CAES technology as "the burned fuel amount per generated peak electricity unit by the expander" [31,32]. Finally, to match the scale of the operation sub-problem with respect to the Master investment problem in one target year, the discount factor f^{dsc} is defined in (4).

3.2 | DC optimal power flow

Power balance constraint for the generated power from generating units, load demand, and the CAES units charging and discharging powers are presented in (5), where the power flow variables are distinguished for the available and the installed transmission lines.

Subject to:

$$\sum_{l=1}^L \left(\beta_{i,l}^{\varphi_0} \cdot \ell_{t,l}^{\varphi_0,ws} + \beta_{i,l}^{\varphi_{1,2}} \cdot \ell_{t,l}^{\varphi_{1,2},ws} \right) + \bar{p}_{t,i}^{g,ws} = \bar{p}_{t,i}^{j,ws} + \bar{p}_{t,i}^{-ws} \quad \forall t, i, ws \quad (5)$$

The DCOPT formulation for the available transmission lines is presented in (6). Note that the DCOPT formulation for the installable transmission lines in the TEP problem formulation is non-linear (7) due to decision variables $\omega_l^{\varphi_{1,2}}$. Therefore, the Big-M method is accordingly applied to linearize this constraint [33,34]. As a result, constraint (7) is replaced by (7a) to prove the linearity in the DCOPT for the installed transmission lines. Note that the parameter Ω in (7a) is set to be ten times of the maximum transmission lines capacity [35]. Finally, the power flow limits for the available and the installed transmission lines and the generated power limits for generating units at bus i are presented in (8)–(10).

$$\ell_{t,l}^{\varphi_0,ws} = \frac{1}{\chi_l} \cdot \omega_l^{\varphi_0} \cdot \theta_{t,l}^{\varphi_0,ws} \quad \forall t, l, ws \quad (6)$$

$$\ell_{t,l}^{\varphi_{1,2},ws} = \frac{1}{\chi_l} \cdot \omega_l^{\varphi_{1,2}} \cdot \theta_{t,l}^{\varphi_{1,2},ws} \quad \forall t, l, ws \quad (7)$$

$$\left| \ell_{t,l}^{\varphi_{1,2},ws} - \frac{\theta_{t,l}^{\varphi_{1,2},ws}}{\chi_l} \right| \leq \Omega \cdot \left(1 - \omega_l^{\varphi_{1,2}} \right) \quad \forall t, l, ws \quad (7a)$$

$$\left| \ell_{t,l}^{\varphi_0,ws} \right| \leq \omega_l^{\varphi_0} \cdot \bar{\ell}_l \quad \forall t, l, ws \quad (8)$$

$$\left| \ell_{t,l}^{\varphi_{1,2},ws} \right| \leq \omega_l^{\varphi_{1,2}} \cdot \bar{\ell}_l \quad \forall t, l, ws \quad (9)$$

$$\underline{\bar{p}}_i^g \leq \bar{p}_{t,i}^{g,ws} \leq \bar{p}_i^g \quad \forall t, i, ws \quad (10)$$

3.3 | CAES units power and energy

The hourly charging and discharging statuses of CAES units is defined in (11). This constraint is particularly related to CAES units due to their efficiency; in other words, by utilizing other ESS technologies with higher efficiency, we would not have required to consider this constraint [36]. Note that the charging and discharging statuses should be dependent on the CAES's integration variable (ψ_i); that is, the binary status values will be non-zero only when CAES units are integrated in the buses (zero elsewhere). Therefore, the CAES units charging and discharging powers capacity limits are non-linear due to the decision variable ψ_i , resulted in non-linear constraints (12), (13).

This paper proposes a novel as well as efficient method to linearize these constraints. In this regard, two new binary variables $\vartheta_{t,i}^{c^{ms}} = \psi_i \cdot v_{t,i}^{c^{ms}}$ and $\vartheta_{t,i}^{d^{ms}} = \psi_i \cdot v_{t,i}^{d^{ms}}$ named CAES units linearizing variables are defined to remove the non-linear terms in (12), (13) and form the final proposed MILP optimization problem. In detail, to connect charging and discharging statuses variables and linearizing variables, two new linear inequalities are suggested in (14), (15).

Reflecting the motivation for the new constraints (14), (15), variables $\vartheta_{t,i}^{c^{ms}}, \vartheta_{t,i}^{d^{ms}}$ are equal to zero when the buses are not reinforced with any CAES units due to their binary structure. Analogously, these variables are binary if CAES units exist on buses. According to our novel linearization method, the coefficients defined and presented in (14), (15) are creatively set as $\sigma_1 = -0.3, \sigma_2 = 0.2, \sigma_3 = 0.4, \sigma_4 = 0.5$ to satisfy the above-mentioned principal purpose of these constraints. A calculation of charging status (14) is shown in (16) to quantify and prove the purpose of the proposed coefficients for the linearization approach. Note that the presented calculation (16) is completely the same for the discharging status. Finally, the constraints (12), (13) are replaced by (12a), (13a) to present the linear charging and discharging powers capacity limits of CAES units.

$$v_{t,i}^{c^{ms}} + v_{t,i}^{d^{ms}} \leq 1 \quad \forall t, i, ws \quad (11)$$

$$0 \leq p_{t,i}^{c^{ms}} \leq \psi_i \cdot v_{t,i}^{c^{ms}} \cdot \bar{p}_i^c \quad \forall t, i, ws \quad (12)$$

$$0 \leq p_{t,i}^{d^{ms}} \leq \psi_i \cdot v_{t,i}^{d^{ms}} \cdot \bar{p}_i^c \quad \forall t, i, ws \quad (13)$$

$$\begin{aligned} & \left(\sigma_1 + \sigma_2 \cdot \left(\psi_i + v_{t,i}^{c^{ms}} \right) \right) \\ & \leq \vartheta_{t,i}^{c^{ms}} \leq \left(\sigma_3 + \sigma_4 \cdot \left(\psi_i + v_{t,i}^{c^{ms}} \right) \right) \quad \forall t, i, ws \end{aligned} \quad (14)$$

$$\begin{aligned} & \left(\sigma_1 + \sigma_2 \cdot \left(\psi_i + v_{t,i}^{d^{ms}} \right) \right) \\ & \leq \vartheta_{t,i}^{d^{ms}} \leq \left(\sigma_3 + \sigma_4 \cdot \left(\psi_i + v_{t,i}^{d^{ms}} \right) \right) \quad \forall t, i, ws \end{aligned} \quad (15)$$

$$\psi_i = \begin{cases} 0 \rightarrow v_{t,i}^{c^{ms}} = 0 \rightarrow -0.3 \leq \vartheta_{t,i}^{c^{ms}} \leq 0.4 \rightarrow \vartheta_{t,i}^{c^{ms}} = 0 \\ 1 \rightarrow v_{t,i}^{c^{ms}} = \begin{cases} 0 \rightarrow -0.1 \leq \vartheta_{t,i}^{c^{ms}} \leq 0.9 \rightarrow \vartheta_{t,i}^{c^{ms}} = 0 \\ 1 \rightarrow +0.1 \leq \vartheta_{t,i}^{c^{ms}} \leq 1.4 \rightarrow \vartheta_{t,i}^{c^{ms}} = 1 \end{cases} \end{cases} \quad (16)$$

$$0 \leq p_{t,i}^{c^{ms}} \leq \vartheta_{t,i}^{c^{ms}} \cdot \bar{p}_i^c \quad \forall t, i, ws \quad (12a)$$

$$0 \leq p_{t,i}^{d^{ms}} \leq \vartheta_{t,i}^{d^{ms}} \cdot \bar{p}_i^c \quad \forall t, i, ws \quad (13a)$$

CAES's energy level per hour and the value of initial energy level in the first hour of the operation sub-problem are defined in (17), (18), while the energy level limit for CAES units is calculated in (19). CAES units' efficiency is modelled based on the

heat rate parameter r^b and the energy ratio parameter r^e [31]. Therefore, different from other ESS technologies, r^e multiplied with the discharging power measures the energy level of CAES units [37]. Note that the energy ratio is specifically defined for CAES technology as "the consumed energy amount by the compressor per the generated energy unit by the expander during the peak hours" [31,32].

$$\delta e_{t,i}^{c^{ms}} = p_{t,i}^{c^{ms}} - r^e \cdot p_{t,i}^{d^{ms}} \quad \forall t \notin \{1\}, i, ws \quad (17)$$

$$e_{t,i}^{c^{ms}} = p_{t,i}^{c^{ms}} - r^e \cdot p_{t,i}^{d^{ms}} \quad \forall t \in \{1\}, i, ws \quad (18)$$

$$0 \leq e_{t,i}^{c^{ms}} \leq \psi_i \cdot \bar{e}_i^c \quad \forall t, i, ws \quad (19)$$

3.4 | Grid-scale system flexibility assessment

Based on [25] in which the authors present a metric for the flexibility assessment, the grid-scale system flexibility metric is obtained from the flexibility power (20) and the value of the initial flexibility power in the first hour of the operation sub-problem (21). The flexibility power is defined as power variations across the system to assess the network capacity to deal with variations. To clarify, the flexibility power depends on two factors: *i*) the capacity of the system generation, and *ii*) the difference at any given time (t) and ($t - 1$) as ramp rates in the generated power from generating units and CAES units' discharging power subtracted from load demand and CAES units' charging power. According to the flexibility concept, which is the ability of the systems to effectively control the variations to daily smooth the generated power and load demand in the operation sub-problem, these two factors have equivalent influences on the grid-scale system flexibility measurement. In other words, as the capacity of the system generation (*i*) can independently improve the system flexibility from hourly time, the proposed difference with generation essence (*ii*) can increase the system flexibility each time of 24-h scale. Therefore, these factors should be multiplied by the same coefficients as the same weight to be normalized and conceptualized the discussed physical meaning ($\rho_1 = \rho_2$).

The flexibility index at bus i at time t in winter/summer days (22) is measured by applying the flexibility power and the maximum capacity of the system generation. The fundamental definition of the system flexibility can be acknowledged by this constraint, in which the effective two factors are cohesively organized in assessing the flexibility index. To quantify the coefficients of the factors in (20), (21), the presented flexibility index (22) can be considered as a metaphor for the system flexibility on the per-unit scale. As the desirable amount of the grid-scale system flexibility is defined to be greater than 0.5 [25], if we supposed there is no variation between given time (t) and ($t - 1$) and the minimum power capacity of generating units is zero, the amount of (22) would be 0.5. Therefore, constraints (20), (21) are forced by the above discussion to consider (0.5)

as the same coefficients for two factors.

$$\begin{aligned} \dot{p}_{t,i}^{f,ws} &= \rho_1 \left(\bar{p}_i^g - \underline{p}_i^g + \bar{p}_i^c \right) \\ &+ \rho_2 \left(\delta \dot{p}_{t,i}^{ws} - \delta \dot{p}_{t,i}^{-ws} - \delta \dot{p}_{t,i}^{ws} \right) \quad \forall t \notin \{1\}, i, ws \end{aligned} \quad (20)$$

$$\begin{aligned} \dot{p}_{t,i}^{f,ws} &= \rho_1 \left(\bar{p}_i^g - \underline{p}_i^g + \bar{p}_i^c \right) \\ &+ \rho_2 \left(\dot{p}_{t,i}^{ws} - \dot{p}_{t,i}^{-ws} - \dot{p}_{t,i}^{ws} \right) \quad \forall t \in \{1\}, i, ws \end{aligned} \quad (21)$$

$$\varepsilon_{t,i}^{ws} = \frac{\dot{p}_{t,i}^{f,ws}}{\bar{p}_i^g + \bar{p}_i^c} \quad \forall t, i, ws \quad (22)$$

Finally, the grid-scale system flexibility metric (23), which is the minimum of the flexibility index at time t in winter/summer days, is defined by considering the weighted sum of the flexibility index (22) at bus i and the capacity of the system generation. It should be noted that the minimum value of the grid-scale system flexibility metric across different time periods and different seasons is conservatively assessed to capture the worst-case scenario in the system.

$$\mathbb{F}_{system} = \min \left\{ \sum_{i=1}^I \left(\varepsilon_{t,i}^{ws} \cdot (\bar{p}_i^g + \bar{p}_i^c) \right) / \sum_{i=1}^I (\bar{p}_i^g + \bar{p}_i^c) \right\} \Big|_{\forall t, ws} \quad (23)$$

3.5 | Contingency scenarios analysis

In order to model the $N - 1$ contingency scenarios, a novel efficient offline mechanism is proposed to repetitively measure the system security under stressed contingency conditions. In this vein, each of the available and the installed transmission lines in each corridor is respectively removed and the load curtailment powers are evaluated. The load curtailment powers are then compared with the corresponding limits in (24); when the load curtailment power in a particular contingency exceeds the desirable limits, this contingency is recorded as a critical scenario. Therefore, the system cannot allow the transmission line to be offline in this particular corridor. Hence, a new constraint, which should reinforce this corridor with another transmission line, is added in order to prevent disconnecting this particular transmission line in the system. Accordingly, the investment plans and the total cost values are updated. This process is repeated independently from the investment problem until all system contingencies are evaluated by considering all the available and the installed transmission lines.

$$\dot{p}_{t,i}^{l,ws} < \dot{p}_{limit}^l \quad \forall t, i, ws \quad (24)$$

4 | THE GARVER CASE STUDY

4.1 | Test system data and assumptions

The 6-bus GARVER test system, comprised of 3 generators and 6 transmission lines, is utilized to demonstrate the functional-

TABLE 1 Investment plans-GARVER test system

	Lines (corridors)	CAES units (buses)
G¹	(2-3) (2-6) (3-5) (4-6) (4-6)	–
G²	(2-6) (2-6) (3-5) (3-5) (4-6) (4-6)	(2) (3) (4) (5) (6)
G³	(2-3) (3-5) (4-6) (4-6)	(1)

TABLE 2 Costs and system flexibility-GARVER test system

	Scenarios		
	G ¹	G ²	G ³
Lines number	5	6	4
CAES units number	0	5	1
Investment (M\$)	130.0	531.5	211.5
Total cost (M\$)	1114.8	1084.9	1090.0
System flexibility	0.457	0.668	0.494

ity of the proposed framework. In this system, the data on the network buses and the available/candidate transmission lines are presented in [21]. Moreover, the hourly profile of the load demand for the daily peaks of two sample winter/summer days is borrowed from [38]. The investment costs are assumed to be 425,000 \$/MW and 53,000 \$/MWh for the power and energy investment costs of the CAES units, respectively [11]. The natural gas cost, heat rate, and energy ratio are considered to be 0.0035 \$/MJ, 4,185 MJ/MWh, and 0.75, respectively [39]. The maintenance costs are assumed to be 1,420 \$/MW*yr and 0.1 \$/MWh for the fixed and variable maintenance costs, respectively [11]. In this case study, the maximum capacities for the power and energy level of the CAES units are assumed 100 MW and 600 MWh, respectively. In addition, the hourly electricity price in electricity consumption is taken from [21]. The limit on the load curtailment power is supposed to be 10 MW. To evaluate the Master investment problem, the annual discount rate is set to 0.12 in a 30-year planning horizon by considering hourly scale of operation sub-problem in each day [40]. Finally, the operation sub-problem is optimized for one target year via the discount factor to determine the winter/summer days in the proposed static co-planning structure.

4.2 | Study results and analysis

All optimization simulations are carried out in the GAMS 24.1.3 environment and via the CPLEX solver on a server PC with a 5-core processor and 8 GB of RAM. Three scenarios are fully analyzed in the studied test system: *i*) TEP studies without the integration of CAES units (G¹), *ii*) TEP studies with the integration of CAES units under $N - 1$ criterion (G²), and *iii*) Analogous to G² with 50% increase in CAES units' investment costs (G³). In this vein, investment plans are presented in Table 1, while the investment, total cost, and the system flexibility are calculated in Table 2.

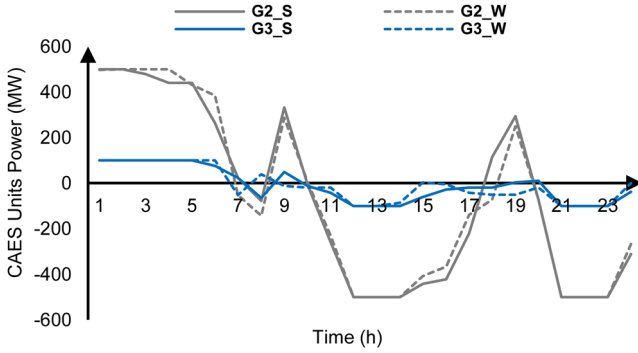


FIGURE 2 Total difference in CAES units charging and discharging powers ($p_{r,i}^{ca}$)-GARVER test system

According to Table 1, new transmission lines are installed in the vulnerable corridors such as 2–6, 3–5, and 4–6, but the worst-case corridor in this system is found to be 4–6 owing to the fact that the most number of possible transmission lines are installed in this corridor. In G^2 compared to G^1 , new transmission lines are installed in corridors 2–6 and 3–5 to satisfy the system load demand under $N - 1$ contingency scenarios. By investigating the effects of the CAES units' investment costs in G^3 , the increase in investment costs decreases the integration of CAES units in this scenario compared to that in G^2 . Also, the integrated CAES units in G^3 help the system to satisfy load demand with lower transmission lines installation as the installed transmission lines in corridor 2–6 are eliminated in comparison with G^1 . Finally, the $N - 1$ contingency has resulted in the increase of the transmission lines installation as well as the CAES units' integration in order to satisfy the system reliability performance requirements.

To investigate the impacts of CAES units' integration on the system flexibility, we precisely analyse the results in Table 2. The number of the installed transmission lines and the integrated CAES units in G^2 is greater than those in G^1 due to the contingency. Moreover, the number of the installed transmission lines in G^3 is lower than that in G^1 due to the integration of CAES units. As the CAES investment costs increase in G^3 , a lower number of CAES units is found to be integrated in the system. The system flexibility and the investment in G^1 is lower compared to other scenarios; also, the total cost is greater than other scenarios since the CAES units are not integrated in this scenario. By considering the integration of CAES units in G^2 , the system flexibility and the investment increase up to $\sim 50\%$ and ~ 402 M\\$ despite the contingency in this scenario, while the total cost decreases down to ~ 30 M\\$ compared to G^1 . Due to the integration of expensive CAES units in G^3 , the system load demand is smoothly satisfied by installing new transmission lines rather than CAES units. As a result, the system flexibility and the investment increase up to $\sim 10\%$ and ~ 82 M\$, while the total cost decreases down to ~ 25 M\\$ compared to G^1 because of the CAES units' integration in G^3 .

As can be seen in Figure 2, CAES units are charged in off-peak hours compared to discharging in peak hours. Due to integrating more CAES units in G^2 , the charging and discharging

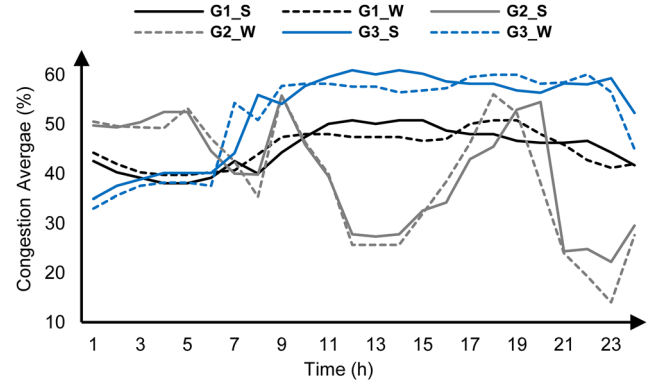


FIGURE 3 The average of the available and the installed transmission lines congestion (%)-GARVER test system

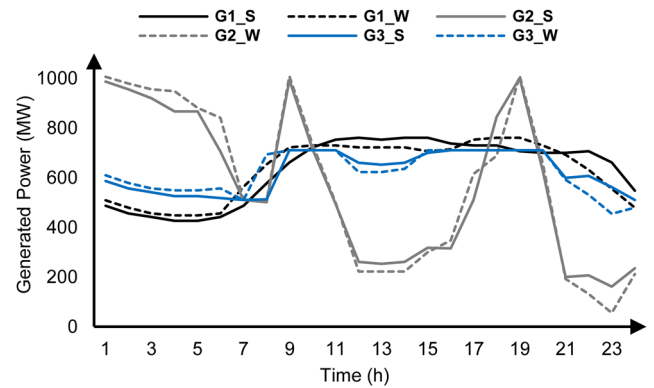


FIGURE 4 Power outputs of generating units-GARVER test system

power of CAES units is significantly more than that in G^3 . Based on Figure 3, transmission lines congestion is declined in G^2 in peak hours by CAES units discharging compared to off-peak hours in which this item is increased by CAES units charging (contrary to G^1 and G^3 with lower CAES units' integration). As a result, integrating CAES units can decline the transmission lines congestion in critical hours to support transmission lines to be not congested in peak hours. Despite the removal of corridor 2–3 in G^2 , transmission lines congestion decreases in comparison with G^1 due to the integration of CAES units as another positive impact of this technology. Finally, power outputs of generating units shown in Figure 4 are decreased in peak hours in G^2 compared to off-peak hours. As a vital conclusion extracted from Figure 4, the integration of CAES units can decrease the generated power of conventional generators and as a result, the operation cost of these generators is decreased by CAES units discharging in critical hours when the cost is huge, while CAES units can be fully charged with more generated power in off-peak hours. To recapitulate, the integration of CAES units can significantly improve the system flexibility, alleviate the need for the installation of new transmission lines, control the transmission lines congestion, decrease the usage of conventional generators, and decline the total cost in both normal as well as contingency states.

TABLE 3 Investment plans-RTS test system

	Lines (corridors)	CAES units (buses)
R^1	(6-10) (8-9) (11-14) (14-16) (14-16) (16-17) (16-17) (17-18)	–
R^2	(6-10) (7-8) (8-9) (11-14) (14-16) (14-16) (16-17) (17-18)	(1) (2) (5) (7) (9) (13) (14) (15) (18) (19) (20)
R^3	(6-10) (7-8) (8-9) (11-14) (11-14) (14-16) (14-16) (15-16) (15-24) (16-17) (17-18)	(2) (3) (7) (9) (10) (14) (16) (19) (20) (21) (24)
R^4	(6-10) (8-9) (11-14) (14-16) (14-16) (16-17) (16-17) (17-18)	(8)

TABLE 4 Costs and system flexibility-RTS test system

	Scenarios			
	R^1	R^2	R^3	R^4
Lines number	8	8	11	8
CAES units number	0	11	11	1
Investment (M\$)	74.8	1703.2	1741.7	268.0
Total cost (M\$)	3293.3	3017.4	3074.3	3287.8
System flexibility	0.398	0.638	0.567	0.419

5 | IEEE RTS CASE STUDY

5.1 | Test system data and assumptions

Commonly applied to evaluate the TEP formulations and reliability evaluation of the transmission systems [41–44], the RTS 24-bus test system—including 10 generators and 38 transmission lines—is utilized to demonstrate the flexibility benefits achieved from the proposed framework. In this system, the data on the network buses and the transmission lines are available in [21], [38]. The investment cost of the transmission lines is assumed to be 1,000 \$/MVA**mile*, while the maximum capacities for the power and energy level of the CAES units are set to 200 MW and 1,200 MWh, respectively. Note that the original test system is very reliable and hence, the maximum power capacity of generating units and load demand are increased to 2.2 times of the original values [21] in order to investigate the performance of the proposed framework on the system flexibility.

5.2 | Study results and analysis

Four scenarios are fully analyzed in the RTS test system: *i*) TEP studies without the integration of CAES units (R^1), *ii*) TEP studies with the integration of CAES units (R^2), *iii*) TEP studies with the integration of CAES units under $N - 1$ criterion (R^3), and *iv*) Analogous to R^3 with 30% increase in the CAES units' investment costs (R^4). The result of the investment plans is shown in Table 3, while Table 4 presents the investment, total cost, and the system flexibility.

According to Table 3, the vulnerable corridors can be easily detected in all four scenarios where new transmission lines are installed; for instance, corridors 6–10, 8–9, 11–14, 14–16, 16–17, and 17–18 are critical in the studied system. Also, the maximum number of transmission lines are installed in corridor 14–16 in all scenarios, which highlights it as the most vulnerable corridor in the system. The removal of one transmission line in corridor 16–17 in R^1 is compensated by installing one transmission line in corridor 7–8 in R^2 . The number of the installed transmission lines in R^3 is greater than that in R^1 and R^2 to fulfil the system load demand under contingency. In this vein, corridors 11–14, 15–16, and 15–24 play a vital role to keep the operation of the system safe under contingencies compared to previous scenarios. The removal of one transmission line in corridor 16–17 in R^3 is compensated by installing one new transmission line in corridor 7–8 similar to that in R^2 . Finally, due to the expensive CAES units integrated in R^4 , the location of new transmission lines is found similar to that in R^1 ; in other words, the system cannot use the expensive CAES units. In addition, buses 2, 7, 9, 14, 19, and 20 are more critical than others, where CAES units are found to be integrated under both normal and contingency states. Changing the location of the integrated CAES units in R^2 and R^3 indicates that the critical buses in the system can change when focusing on a normal or contingency state. Moreover, the integration of CAES units in R^4 has declined in comparison with that in R^2 and R^3 .

We precisely scrutinize Table 4 in order to investigate the impacts of CAES units' integration on the system flexibility in the RTS test system. In this regard, the total installed transmission lines in R^2 is equal to that in R^1 , while the integration of CAES units has decreased the transmission lines congestion that will be precisely discussed in Figure 6. The total number of the installed transmission lines and the integrated CAES units in R^3 are greater than those in R^1 in order to satisfy the $N - 1$ reliability criterion; also, the number of the installed transmission lines has increased in R^3 compared to that in R^2 . Finally, the increase of the CAES units' investment costs in R^4 confirms that the expensive CAES units may not significantly affect the system and as a result, the number of the installed transmission lines in this scenario is similar to that in R^1 , while the number of the integrated CAES units has decreased in comparison with that in R^2 and R^3 .

To investigate the CAES units' integration in the system, we here present the effectiveness of the CAES units on the total cost and the system flexibility. The investment and system flexibility are in their lowest level in R^1 , while the total cost is in its highest value compared to other scenarios. In R^2 , where CAES units are integrated, the system flexibility and the investment increase up to ~60% and ~1628 M\$, while the total cost decreases down to ~276 M\$ in comparison with that in R^1 . By considering the CAES units' integration and the $N - 1$ reliability criterion in R^3 , the system flexibility as well as the investment increase, while the total cost decreases in comparison with R^1 . However, the system flexibility decreases down to ~10% and the investment as well as the total cost increase up to 39 M\$ and 57 M\$ compared to R^2 , primarily in response to the contingency. In R^4 , similar to the GARVER test system results,

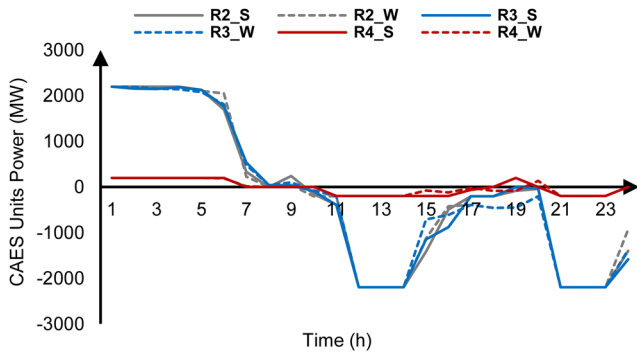


FIGURE 5 Total difference in CAES units charging and discharging powers ($p_{r,i}^{wt}$)-RTS test system

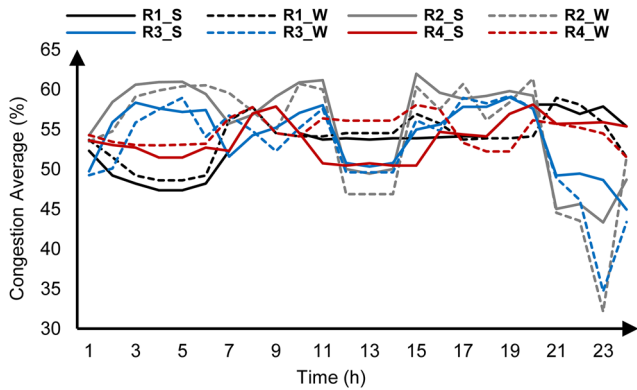


FIGURE 6 The average of the available and the installed transmission lines congestion (%)-RTS test system

the load demand is smoothly satisfied by installing the transmission lines rather than integrating the CAES units. Therefore, in comparison with R^1 , the system flexibility and the investment increase up to $\sim 5\%$ and ~ 193 M\$, while the total cost decreases down to ~ 6 M\$. Furthermore, the system flexibility (decreasing down to $\sim 26\%$), the investment (decreasing down to 1474 M\$), and the total cost (increasing up to ~ 214 M\$) in R^4 are different than those in R^3 , demonstrating the lower integration of the expensive CAES units in R^4 .

According to Figure 5, CAES units are charged in off-peak hours, while discharging in peak hours. In detail, the charging and discharging powers of CAES units in R^3 are slightly more than R^2 due to the contingencies. Because of integrating more CAES units in R^2 and R^3 , the powers of CAES units are significantly more than those in R^4 . Considering Figure 6, by discharging in peak hours, transmission lines congestion is declined in R^2 and R^3 compared to off-peak hours that transmission lines congestion is increased by CAES units charging. Conversely, with lower CAES units' integration in R^1 and R^4 , transmission lines congestion is increased in peak hours, while being decreased in off-peak hours. As a result, the transmission lines congestion can be efficiently managed in peak hours by CAES units' integration. On the other hand, the placement of the installed transmission lines in R^2 is approximately similar to that in R^1 (Table 3), but the transmission lines congestion in peak hours has decreased in R^2 compared to R^1 primarily due to the integration of CAES units.

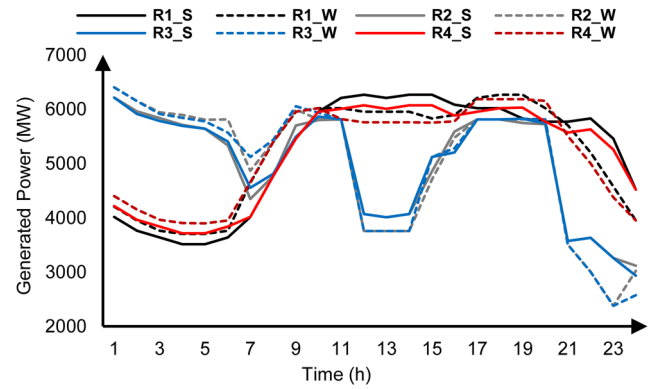


FIGURE 7 Power outputs of generating units-RTS test system

Based on Figure 7, power outputs of generating units in R^2 and R^3 are decreased in peak hours, while these items are increased in R^1 and R^4 due to lower CAES units' integration. Therefore, the generated power of conventional generators and thus, the operation cost of the generators can be bounded by the integration of CAES units which are discharged in critical hours. Moreover, all the integrated CAES units in the system can be fully charged by more conventional generators in off-peak hours. To summarize, the integration of CAES units in TEP studies can considerably improve the system flexibility, while it can reduce the need for installing new transmission lines, transmission lines congestion, the usage of conventional generators, and the total cost in both normal and contingency states. In this vein, although initial investment on CAES units would be costly, the investments can be economically justified considering the significant benefits (cost reduction) achieved in both case studies. Since TEP studies are inevitable in power systems planning, part of the earned income from cost reduction in CAES-integrated power grids can be granted to investors as one of the incentive options. As a result, this technology can play a substantial role in the future of the modern power systems when planning to expand the network with modern technologies.

6 | CONCLUSION

This paper presented a novel mathematical linearized model to capture the impacts of CAES units' integration on the system flexibility considering the co-planning of this modern technology and the TEP analysis. The Big-M method and an innovative approach were effectively implemented to translate the non-linear model into a MILP optimization formulation for TEP and CAES units. Also, a new metric of the grid-scale system flexibility was introduced to numerically evaluate the system performance when integrating the optimized plans. In order to satisfy the system security under contingency scenarios, a new repetitive computationally attractive offline mechanism was investigated to evaluate the $N - 1$ reliability criterion. The proposed model was applied to the GARVER 6-bus test system and the RTS 24-bus test system. Techno-economic evaluation of the proposed analytics demonstrated the effectiveness: it was shown that the CAES units can improve the system

flexibility, relax or postpone the need for construction and installation of new transmission lines, control the transmission lines congestion, decrease the usage of conventional generators, and reduce down the system total cost. Future research could be focused on the application of the proposed framework to RES-integrated power systems considering different ESS technologies (e.g. BESS units) and capturing the prevailing uncertainties in RES.

ACKNOWLEDGEMENTS

This work was supported in part by INSF.

CONFLICT OF INTEREST

The authors have declared no conflict of interest.

NOMENCLATURE

Indices and Sets

- i, I Index and number of buses.
- l, L Index and number of transmission lines.
- t, T Index of time in daily scale $\{1, \dots, 24\}$.
- φ_0 Index of the available transmission lines.
- $\varphi_{1,2}$ Index of first and second candidate transmission lines.
- ws, Y Index and number of winter/summer days.
- n, N Index and number of defined periods to match the operation scale with the investment in one target year.

Parameters

- α^l Investment cost of transmission line l (\$/MVA*mile).
- α^p, α^e Investment power (\$/MW) and energy (\$/MWh) costs of CAES units, respectively.
- α^f, α^v Fixed (\$/MW*yr) and variable (\$/MWh) maintenance costs.
- α_i^g Operation cost of generating units at bus i (\$/MWh).
- α_t^e Electricity price at time t (\$/MWh).
- α^{ng} Natural gas cost (\$/MJ).
- $\omega_l^{\varphi_0}$ Binary parameter of the available transmission line $l \in \{0, 1\}$.
- ζ^{ws} Number of winter/summer days in one target year.
- $\beta_{i,l}^{\varphi_0}, \beta_{i,l}^{\varphi_{1,2}}$ Matrices for connecting the available and the candidate transmission line l to bus i , respectively.
- $\hat{p}_{t,i}^{ws}$ Load demand at bus i at time t in winter/summer days (MW).
- χ_l Transmission line l reactance (P.U).
- $\bar{\ell}_l$ Maximum power flow capacity of transmission line l (MVA).
- $\underline{\hat{p}}_i^g, \bar{\hat{p}}_i^g$ Minimum and maximum power capacity of generating units at bus i , respectively (MW).
- \bar{p}_i^c, \bar{e}_i^c Maximum power (MW) and energy (MWh) capacity limits for CAES units at bus i , respectively.
- r^h, r^e Heat rate (MJ/MWh) and energy ratio of CAES units, respectively.
- r^{disc}, f^{disc} Discount rate and discount factor, respectively.
- Ω Big number in Big-M method.
- \bar{p}_{limit}^c Load curtailment power limit (MW).

Continuous Variables

- C_{pl} Investment cost of the installed transmission lines and the integrated CAES units (\$).
- C_{op}^{ws} Operation cost of generating units and the integrated CAES units in winter/summer days (\$).
- $\hat{p}_{t,i}^{gws}$ Output power of generating units at bus i at time t in winter/summer days (MW).
- $\hat{p}_{t,i}^{cws}, \hat{p}_{t,i}^{dws}$ CAES units charging and discharging powers at bus i at time t in winter/summer days, respectively (MW).
- $\hat{p}_{t,i}^{+ws}$ Total summation of CAES units charging and discharging powers $\{\hat{p}_{t,i}^{cws} + \hat{p}_{t,i}^{dws}\}$ at bus i at time t in winter/summer days (MW).
- $\hat{p}_{t,i}^{-ws}$ Total difference in CAES units charging and discharging powers $\{\hat{p}_{t,i}^{cws} - \hat{p}_{t,i}^{dws}\}$ at bus i at time t in winter/summer days (MW).
- $\hat{p}_{t,i}^{fxws}$ Flexibility power at bus i at time t in winter/summer days (MW).
- $\delta(\bullet)$ The subtraction of a parameter/variable at time t and $t - 1$. e.g. $\delta \hat{p}_{t,i}^{cws} = \hat{p}_{t,i}^{cws} - \hat{p}_{t-1,i}^{cws}$
- $\hat{p}_{t,i}^{cws}$ Load curtailment power at bus i at time t in winter/summer days (MW).
- $e_{t,l}^{\varphi_0ws}, e_{t,l}^{\varphi_{1,2}ws}$ Power flow of the available and the installed transmission line l at time t in winter/summer days (MW), respectively.
- $\theta_{t,l}^{\varphi_0ws}, \theta_{t,l}^{\varphi_{1,2}ws}$ Voltage phase angle difference between two buses, connecting the available and the installed transmission line l at time t , respectively.
- $e_{t,i}^{cws}$ The energy level of CAES units at bus i at time t in winter/summer days (MWh).
- $\varepsilon_{t,i}^{ws}$ Flexibility index at bus i at time t in winter/summer days.
- \mathbb{F}_{system} Grid-scale system flexibility metric.

Binary Variables



- $\omega_l^{\varphi_{1,2}}$ Binary variables of first and second installed transmission line l .
- ψ_i Binary variable of the integrated CAES units at bus i .
- $v_{t,i}^{cws}, v_{t,i}^{dws}$ Binary variables to define CAES units charging and discharging statuses at bus i at time t in winter/summer days, respectively.
- $\vartheta_{t,i}^{cws}, \vartheta_{t,i}^{dws}$ CAES units linearizing binary variables in the proposed linearization method for charging and discharging statuses at bus i at time t in winter/summer days, respectively.

ORCID

Hesam Mazaheri  <https://orcid.org/0000-0002-4115-5784>

Moein Moeini-Aghataie  <https://orcid.org/0000-0002-7656-6807>

Mahmud Fotuhi-Firuzabad  <https://orcid.org/0000-0002-5507-9938>

Payman Dehghanian  <https://orcid.org/0000-0003-2237-4284>
 Mohammad Khoshjahan  <https://orcid.org/0000-0002-3281-4936>

REFERENCES

- Heydarian-Forushani, E., Golshan, M.E.H., Siano, P.: Evaluating the operational flexibility of generation mixture with an innovative techno-economic measure. *IEEE Trans. Power Syst.* 33(2), 2205–2218 (2018)
- Majzoubi, A., Khodaei, A.: Application of microgrids in supporting distribution grid flexibility. *IEEE Trans. Power Syst.* 32(5), 3660–3669 (2017)
- Morales-Espana, G., Tejada-Arango, D.A.: Modelling the hidden flexibility of clustered unit commitment. *IEEE Trans. Power Syst.* 34(4), 3294–3296 (2019)
- Anwar, M.B., et al.: Harnessing the flexibility of demand-side resources. *IEEE Trans. Smart Grid* 10(4), 4151–4163 (2019)
- Mazaheri, H., et al.: Expansion planning of transmission networks. In: Zobaa, A. F. (ed.) *Uncertainties in Modern Power Systems*, pp. 35–56. Elsevier, New York (2020)
- Mohandes, B., et al.: A review of power system flexibility with high penetration of renewables. *IEEE Trans. Power Syst.* 34(4), 3140–3155 (2019)
- Khoshjahan, M., et al.: Advanced bidding strategy for participation of energy storage systems in joint energy and flexible ramping product market. *IET Gener. Transm. Distrib.* 14(22), 5202–5210 (2020)
- Karthikeyan, N., et al.: Predictive control of flexible resources for demand response in active distribution networks. *IEEE Trans. Power Syst.* 34(4), 2957–2969 (2019)
- Konstantelos, I., Strbac, G.: Valuation of flexible transmission investment options under uncertainty. *IEEE Trans. Power Syst.* 30(2), 1047–1055 (2015)
- Liang, L., Hou, Y., Hill, D.J.: GPU based enumeration model predictive control of pumped storage to enhance operational flexibility. *IEEE Trans. Smart Grid* 10(5), 5223–5233 (2019)
- Connolly, D.: A review of energy storage technologies: for the integration of fluctuating renewable energy. Dissertation, Limerick University (2010)
- Hozouri, M.A., et al.: On the use of pumped storage for wind energy maximization in transmission-constrained power systems. *IEEE Trans. Power Syst.* 30(2), 1017–1025 (2015)
- Jabr, R.A.: Optimization of AC transmission system planning. *IEEE Trans. Power Syst.* 28(3), 2779–2787 (2013)
- Mazaheri, H., et al.: Investigating the impacts of energy storage systems on transmission expansion planning. In: *Iranian Conference on Electrical Engineering*, Tehran, pp. 1199–1203 (2017)
- Zhang, X., Conejo, A.J.: Coordinated investment in transmission and storage systems representing long- and short-term uncertainty. *IEEE Trans. Power Syst.* 33(6), 7143–7151 (2018)
- Orfanos, G.A., Georgilakis, P.S., Hatzigiorgiou, N.D.: Transmission expansion planning of systems with increasing wind power integration. *IEEE Trans. Power Syst.* 28(2), 1355–1362 (2013)
- Jabr, R.A.: Robust transmission network expansion planning with uncertain renewable generation and loads. *IEEE Trans. Power Syst.* 28(4), 4558–4567 (2013)
- Alizadeh, B., et al.: Robust transmission system expansion considering planning uncertainties. *IET Gener. Transm. Distrib.* 7(11), 1318–1331 (2013)
- Qiu, T., et al.: Stochastic multi-stage co-planning of transmission expansion and energy storage. *IEEE Trans. Power Syst.* 32(1), 643–651 (2017)
- Falugi, P., Konstantelos, I., Strbac, G.: Planning with multiple transmission and storage investment options under uncertainty: A nested decomposition approach. *IEEE Trans. Power Syst.* 33(4), 3559–3572 (2018)
- Mazaheri, H., et al.: An online method for MILP co-planning model of large-scale transmission expansion planning and energy storage systems considering $N - 1$ criterion. *IET Gener. Transm. Distrib.* 15(4), 664–677 (2021)
- Lannoye, E., Flynn, D., O'Malley, M.: Evaluation of power system flexibility. *IEEE Trans. Power Syst.* 27(2), 922–931 (2012)
- Lannoye, E., Flynn, D., O'Malley, M.: Transmission, variable generation, and power system flexibility. *IEEE Trans. Power Syst.* 30(1), 57–66 (2015)
- Nosair, H., Bouffard, F.: Flexibility envelopes for power system operational planning. *IEEE Trans. Sustainable Energy* 6(3), 800–809 (2015)
- Ma, J., et al.: Evaluating and planning flexibility in sustainable power systems. *IEEE Trans. Sustainable Energy* 4(1), 200–209 (2013)
- Zhao, J., Zheng, T., Litvinov, E.: A unified framework for defining and measuring flexibility in power system. *IEEE Trans. Power Syst.* 31(1), 339–347 (2016)
- Pourahmadi, F., et al.: Dynamic uncertainty set characterization for bulk power grid flexibility assessment. *IEEE Syst. J.* 14(1), 718–728 (2020)
- Moreira, A., et al.: A five-level MILP model for flexible transmission network planning under uncertainty: A Min–Max regret approach. *IEEE Trans. Power Syst.* 33(1), 486–501 (2018)
- Zidar, M., et al.: Review of energy storage allocation in power distribution networks: Applications, methods and future research. *IET Gener. Transm. Distrib.* 10(3), 645–652 (2016)
- Dvorkin, Y., et al.: Ensuring profitability of energy storage. *IEEE Trans. Power Syst.* 32(1), 611–623 (2017)
- Shafiee, S., et al.: Risk-constrained bidding and offering strategy for a merchant compressed air energy storage plant. *IEEE Trans. Power Syst.* 32(2), 946–957 (2017)
- Drury, E., Denholm, P., Sioshansi, R.: The value of compressed air energy storage in energy and reserve markets. *Energy* 36(8), 4959–4973 (2011)
- Villumsen, J.C., Bronmo, G., Philpott, A.B.: Line capacity expansion and transmission switching in power systems with large-scale wind power. *IEEE Trans. Power Syst.* 28(2), 731–739 (2013)
- Tohidi, Y., et al.: Coordination of generation and transmission development through generation transmission charges—A game theoretical approach. *IEEE Trans. Power Syst.* 32(2), 1103–1114 (2017)
- Chen, B., et al.: Robust optimization for transmission expansion planning: Minimax cost vs. minimax regret. *IEEE Trans. Power Syst.* 29(6), 3069–3077 (2014)
- Zhao, B., Conejo, A.J., Sioshansi, R.: Using electrical energy storage to mitigate natural gas-supply shortages. *IEEE Trans. Power Syst.* 33(6), 7076–7086 (2018)
- Shafiee, S.: Optimal operation planning of compressed air energy storage plants in competitive electricity markets. Dissertation, University of Calgary (2017)
- Grigg, C., et al.: The IEEE reliability test system-1996. A report prepared by the reliability test system task force of the application of probability methods subcommittee. *IEEE Trans. Power Syst.* 14(3), 1010–1020 (1999)
- Safaei, H., Keith, D.W.: Compressed air energy storage with waste heat export: An Alberta case study. *Energy Conversion & Management* 78, 114–124 (2014)
- Mazaheri, H.: Incorporating the impacts of energy storage systems on transmission expansion planning studies. Dissertation, Sharif University of Technology (2017)
- Ahmadi, S., et al.: Dynamic robust generation–transmission expansion planning in the presence of wind farms under long- and short-term uncertainties. *IET Gener. Transm. Distrib.* 14(23), 5418–5427 (2020)
- Gupta, N., et al.: A bi-level evolutionary optimization for coordinated transmission expansion planning. *IEEE Access* 6, 48455–48477 (2018)
- Li, C., et al.: Flexible transmission expansion planning associated with large-scale wind farms integration considering demand response. *IET Gener. Transm. Distrib.* 9(15), 2276–2283 (2015)
- Ranjbar, H., Hosseini, S.H.: Stochastic multi-stage model for co-planning of transmission system and merchant distributed energy resources. *IET Gener. Transm. Distrib.* 13(14), 3003–3010 (2019)

How to cite this article: Mazaheri, H., et al.: A linearized transmission expansion planning model under $N - 1$ criterion for enhancing grid-scale system flexibility via compressed air energy storage integration. *IET Gener. Transm. Distrib.* 16, 208–218 (2022). <https://doi.org/10.1049/gtd2.12226>